On the limits of optical interconnects

N. Davidson, A. A. Friesem, and E. Hasman

The density capabilities of free-space optical interconnects are analyzed by applying Gabor's theory of information. It is shown that it is possible to increase the space–bandwidth product capabilities of space-variant interconnect schemes if they have symmetry properties. Several examples of such symmetries (locality, separability and smoothness) are discussed in detail, together with some experimental results.

I. Introduction

Free-space optical interconnects are attractive for both analog and digital–optical computers because of their low cross talk, high bandwidth, and parallel operation. A key criterion for the usefulness of such interconnects is their space–bandwidth product (SBP) capability. This criterion determines, to a large extent, the computational performance of an optical computer, and therefore has been investigated in some detail.[1–5] These investigations showed that for an input containing N distinct resolution cells (pixels) the required number of degrees of freedom is N^2 in the space-variant case, whereas it is only N in the space-invariant case.[5] Since, according to Gabor's information theory, the total number of degrees of freedom for any optical system is governed by its size[6] the SBP capabilities of space-variant interconnects are far lower than those of space-invariant ones.

Here we introduce interconnects with certain symmetry properties that cannot be classified as either wholly space-variant or wholly space-invariant. In accordance with Gabor's theory of information[6] we show how these symmetries can be exploited so as to improve the SBP capabilities of interconnects. We begin by presenting the basic relations that are useful for analyzing interconnects with symmetry properties, and the present interconnects with three types of symmetries, namely locality, separability, and smoothness. The analysis is applicable both to continuous (analog) as well as to discrete (digital) interconnect schemes, although continuous notation is used to describe the interconnects throughout this paper. Here the interconnect arrangements can be regarded as optical coordinate transformation.[7]

II. Basic Relations

A basic relation of Gabor's theorem on light and information[6] indicates that any linear optical system has a finite number of degrees of freedom F, which is expressed by

$$F = A\Omega/\lambda^2, \tag{1}$$

where A is the area of the optical beam, Ω is the solid angle of the beam spread, and λ is the optical wavelength. Several constant factors of the order of 1, that depend on the particular implementations may be added to Eq. (1); for example, a constant factor of 2 (or 4) should be added to the right side of Eq. (1) in cases in which phase (and polarization) are exploited for information coding. Such constant factors are therefore omitted in our equations.

The amount of information (in bits) that may be carried in each degree of freedom is given by $\log_2(1 + s/n)$, where s/n is the signal-to-noise ratio. The physical origin of Gabor's theorem is diffraction. Any attempt to increase the resolution of an information cell beyond the limits imposed by diffraction is accompanied by a corresponding exponential decrease in the s/n ratio so as to maintain the total information capacity consistent with Gabor's theorem. Typical examples that show such a behavior are super resolution[8] and near-field microscopy.[9] In the context of interconnect configurations, we thus should seek an approach for increasing the information capacity of interconnects by enlarging the number of available channels without a corresponding decrease in the s/n ratio.

Now the number of degrees of freedom of an optical

The authors are with the Department of Electronics, Weizmann Institute of Science, P.O. Box 26, Rehovot 76100, Israel.

Received 10 June 1991.
0003-6935/92/265426-05$05.00/0.

© 1992 Optical Society of America.

interconnect system may be intuitively expressed as[4,5]

$$F = MN, \tag{2}$$

where N is the number of pixels that are transformed by the system (the SBP), and M is the number of different types of operation or, equivalently, the number of different point-spread functions.[10] The concept of a type of operation is central for understanding the limitations imposed on optical interconnects and is explained in some detail below. Here we illustrate it with a simple example in which we compare wholly space-variant and wholly space-invariant linear optical operations.

Space-invariant linear optical operations, such as simple imaging, may be described mathematically as a convolution of the light amplitudes at the input with some point-spread function that is independent of the input coordinates. The same operation is performed on each pixel in the input, so the number of types of operation is $M = 1$. In computation theory this kind of interconnect operation is referred as cellular automata.[11] The SBP, according to Eqs. (1) and (2), is then $N = A\Omega/\lambda^2$, in agreement with the SBP of an aberration-free imaging system. On the other hand, a general space-variant linear optical operation is described as an integration of the light amplitude at the input multiplied by a kernel that is a function of both the input and the output coordinates.[5] Here a different type of operation is performed on each pixel in the input, so the number of types of operation becomes $M = N$. The resulting SBP is then the square root of that for space-invariant operations.[5] This simple example explains why the value of the SBP for high-quality imaging lenses is typically several thousands in each spatial dimension, whereas that for space-variant interconnect schemes is usually less than a hundred.

In general, however, M may take an intermediate value between 1 and N. For example, two-dimensional perfect shuffle and inverse transformations involve $M = 4$ different types of operation,[12,13] and, strictly speaking, are regarded as space-variant operations. Nevertheless, the fundamental limit on the SBP capabilities is $N = F/4$, which is much greater than the $N = F^{1/2}$ limit for a general space-variant operation. Of course, only optical implementations that take advantage of the degeneracy of the operation can actually reach the improved limit.[12,13] Other implementations that treat the perfect shuffle and its inverse as regular crossbar transformations[14] are still restricted by the much lower $F^{1/2}$ limit.

Below we present several examples of possible symmetries in optical interconnects. For each symmetry we determine the limits of the possible SBP capabilities, and illustrate actual optical implementations that may achieve these limits.

III. Locality

Consider a coordinate transformation (CT) for a two-dimensional function $t(x, y)$ of the form

$$t(x, y) \rightarrow t[u(x, y), v(x, y)], \tag{3}$$

where $u(x, y)$ and $v(x, y)$ are the new coordinates. In the discrete case such a CT corresponds to an interconnect scheme with a fan-out of 1, which is also referred to as the optical crossbar. An optical implementation of such a CT, which was first suggested by Bryngdahl,[7] included a holographic optical element (HOE) and a Fourier transform lens between the input and the output. The SBP capabilities of this implementation, in which a paraxial approximation is used, are given as[15]

$$N = \frac{\sqrt{A}}{\lambda f_{\#}}, \tag{4}$$

where $f_{\#}$ is the focal number of the lens. For a square aperture $f_{\#}^{-2}$ corresponds to the solid angle Ω of Eq. (1) in the paraxial case, and Eq. (4) essentially gives the expected SBP for a general space-variant operation.

So far we have made no assumption on the properties of the CT. Specifically, global connectivity was allowed, and any pixel in the input might have been transformed to any pixel in the output. We now consider transformations that allow local connectivity only. We define the amount of local connectivity by a dimensionless number η,

$$\eta = \Delta_{\max}/D, \tag{5}$$

where $\Delta_{\max} = [(u - x)^2 + (v - y)^2]^{1/2}$ is the maximal lateral displacement of the CT, and D is a typical width of the input; for a square input $D = \sqrt{A}$. A CT with local connectivity of η can transform each pixel in the input to only one of the $\eta^2 N$ pixels in the output, where N is the total number of pixels to be determined. Thus the number of different types of operation is now

$$M = \eta^2 N. \tag{6}$$

To find the SBP capabilities of this CT we resort to Gabor's theorem. Incorporating Eq. (6) into Eq. (2) yields the maximal SBP as

$$N = \sqrt{F}/\eta. \tag{7}$$

For CT's with global connectivity $\eta = 1$, the SBP capabilities of Eq. (7) reduce to that of a general space-variant optical operation. On the other hand, for CT's with highly localized connectivity $\eta \ll 1$ the SBP capabilities are improved considerably. Note that Eq. (7) holds for $\eta > F^{-1/2}$ only; for smaller values of η the system may be considered as space invariant, and its SBP capabilities are determined by Eq. (1) with $N = F$.

Recently we presented an improved optical implementation for achieving the transformation of Eq. (4) (see Ref. 15). No Fourier transform lens was needed, and the locality of the CT was exploited to decrease the distance between the input and the output planes, and thereby to decrease the minimal pixel size. On the grounds of the diffraction theory, we calculated the SBP capabilities of our implementation and found that they were equal to the fundamental limit imposed by Eq. (7). A similar approach was also suggested by Feldman *et al.*[3] and applied by them to the basis set configuration.

IV. Separability

We now consider another possible symmetry in two-dimensional CT's, namely, separability between the x and y dimensions. A separable CT may be expressed as

$$t(x, y) \rightarrow t[u(x), v(y)]. \tag{8}$$

This transformation can be separated into two stages, with only one spatial coordinate being transformed in each stage. We present an optical implementation for the first stage only, $t(x, y) \mapsto t[u(x), y]$; the second stage may be implemented by an identical optical arrangement that is placed in cascade with the first. Here there is a degeneracy among all the pixels that have the same x coordinate. Therefore, the number of different types of optical operation is only $m = \sqrt{N}$. Incorporating this value into Eq. (2) yields the maximal SBP capabilities for the separable CT as

$$N = F^{2/3}. \tag{9}$$

For optical systems with many degrees of freedom, the increase from the power of 1/2 for general CT's to the power of 2/3 for separable CT's offers a substantial improvement. For example, with a 5 cm × 5 cm input and visible light ($\lambda \approx 0.5$ μm), the number of degrees of freedom is $F \approx 10^{10}$. Here, the SBP capabilities increase because of separability by a factor of ~50.

In order to achieve the SBP capabilities of Eq. (9), it is necessary for the optical implementation to exploit the degeneracy of the CT. Thus the first stage of the CT of expression (8) is separated into two steps (a total of four steps for the whole CT). In the first step the input is divided into $M = \sqrt{N}$ groups, each needing the same kind of operation. Then, in the second step, the operation is performed simultaneously on all the pixels within each group. This may be done with the optical arrangement shown schematically in Fig. 1. The operation of each step is performed with a HOE and a Fourier lens. The input, the Fourier, and the output planes are all assumed to be squares with a size of $D \times D$.

The first HOE is composed of $\sqrt{N}$ subholograms, each of which is located adjacent to one column on the input; the size of each subhologram is $D \times D/\sqrt{N}$. Each subhologram comprises a linear grating with a period and an orientation that is different from all the gratings in the other subholograms. Thus the first step of the optical arrangement encodes the columns of the input and directs all the pixels within each column to the same location in the Fourier plane (in our case these locations are arranged as a square matrix). Thus the entire Fourier plane can be fully utilized. This encoding may be viewed as an extension of Lohmann's theta modulation concept,[16] in which only the orientation of the grating is changed from one subhologram to the other.

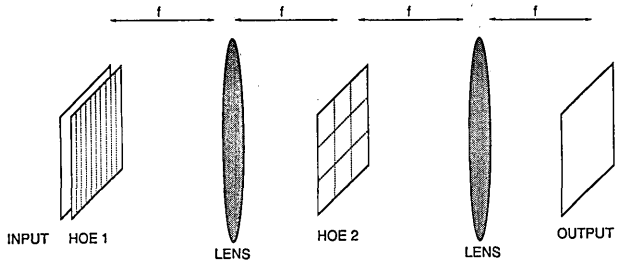

Fig. 1. Optical arrangement for implementing the first stage of a two-dimensional separable CT.

The second hologram, which is located in the Fourier plane of the input, is also composed of $\sqrt{N}$ subholograms, but these are arranged in a square matrix of $(N)^{1/4} \times (N)^{1/4}$. Each of these subhologram transforms a column x_0 from the input into a column $u(x_0)$ at the output. Thus the grating functions of the subholograms are linear, with the form

$$\phi_x(x_f, y_f) = \frac{2\pi}{\lambda} \frac{u(x_0) - x_0}{f} x_f, \tag{10}$$

where (x_f, y_f) are the coordinates at the Fourier plane, and f is the focal distance of the Fourier lens.

The optical arrangement of Fig. 1 was tested experimentally for performing a one-dimensional logarithmic CT on a two-dimensional input, as given by

$$t(x, y) \mapsto t[x, (y + \ln x)]. \tag{11}$$

For the purpose of clarity, the columns of the input were shifted vertically instead of horizontally, as would be required by expression (8). The input was a 20 mm × 20 mm transparency that contained a matrix of 64 × 64 square black transparent pixels ($N = 4096$), and the focal distances of the two lenses were 560 mm. The HOE's were recorded as Lee-type computer-generated holograms[17] and the illumination source was an argon laser ($\lambda = 514.5$ nm). An off-axis linear term was added to the grating function of both HOE's in order to separate the first diffraction order from the undesired ones. The results of the experiment are shown in Fig. 2. It shows the output with two separate images representing the zeroth and first diffracted orders of the second HOE. The left image (the zeroth order) is simply the telescopic image of the input, while in the right image (first order) the columns are indeed shifted vertically (the y direction) by a distance proportional to the logarithm of x. As is evident, the pixels in each image, although distorted somewhat by the transfor-

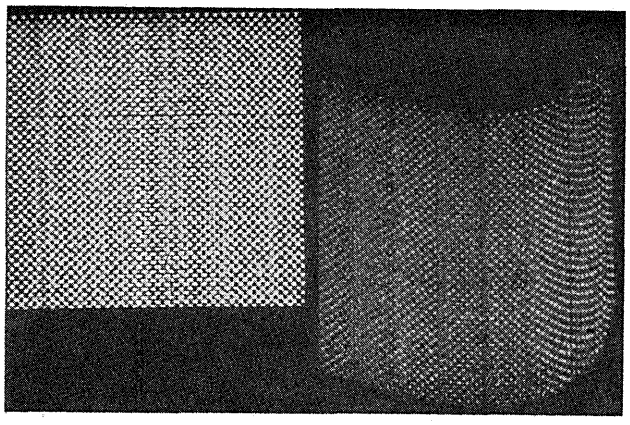

Fig. 2. Experimental results of a one-dimensional logarithmic CT on a two-dimensional input. The telescopic image of the input is shown on the left and the corresponding transformed output is shown on the right. The actual size for all is 20 mm × 20 mm.

mation, are still clearly separated and well defined. The SBP that is demonstrated here is 4096 pixels, which is not far from the fundamental limit of ~6000 pixels, as derived from Eqs. (1) and (9).

V. Smoothness

In the sections above we illustrated how to improve the SBP capabilities of optical interconnects by exploiting the symmetries of the interconnect pattern. In the examples given, the symmetries were obvious and the amount of degeneracy (the ratio between the number of pixels N and the number of different types of optical operations M) was easily determined. Specifically the concept of a type of operation was interpreted as the lateral displacement between the pixel's location in the input and its location in the output. However, it may also be possible to exploit less obvious symmetries, or, in other words, less obvious basic types of optical operation. We illustrate such possibilities by considering the smoothness of the interconnect as a kind of symmetry, and a uniform magnification combined with lateral displacement (off-axis imaging) as a basic type of optical operation. For simplicity we present one-dimensional transformations, but the procedure can be readily extended to two-dimensional transformations.

Consider the one-dimensional CT of $t(x) \mapsto t[u(x)]$, where the input and output are defined over the section $(0, D)$. It is convenient to express $u(x)$ as

$$u(x) = Du_0(x/D), \tag{12}$$

where the dimensionless function u_0 transforms the section (0, 1) upon itself. A possible arrangement for performing the transformation is schematically shown in Fig. 3 It includes two stages. The first stage divides the input into sections with size Δ (to be determined later), and images each section $(x_0, x_0 + \Delta)$ to a section $[u(x_0), u(x_0 + \Delta)]$ in a linear approximation to the desired transformation $u(x)$. Note that the shift and magnification are uniform for each section (although these differ from one section to another); hence, the optical operation on each section

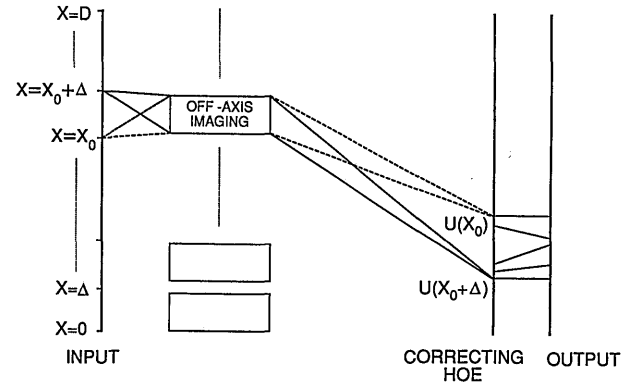

Fig. 3. Optical arrangement for implementing a one-dimensional smooth CT. Some of the rays that emerge from section $(x_0, x_0 + \Delta)$ are shown.

is space invariant. The maximal deviation between the linear transformation of the first stage and the desired nonlinear one $u(x)$ may be approximated by the second term in a Taylor series, which is given by

$$\delta u \approx \frac{u_0''\Delta^2}{2D}, \tag{13}$$

where u_0'' is the maximal second derivative of u_0 and higher derivatives were neglected. This deviation may be referred to as the aberration in the CT that results from the first stage.

In the second stage the aberrations of the first stage are corrected by exploiting a space-variant, but highly localized, CT. Such a localized CT can have high SBP capabilities, as explained in Section II.

To determine the SBP capabilities of the entire CT we begin by calculating separately the minimal pixel size p that may be transformed by each stage without degradation. In the first space-invariant stage the regular diffraction limit relation gives the minimal pixel size as

$$p_1 \approx \lambda f_{\#} = \lambda f/\Delta \approx \lambda D/\Delta, \tag{14}$$

where the focal distance of the imaging system f was assumed equal to D. In the second space-variant stage the minimal pixel size is[15]

$$p_2 \approx [\lambda(\delta u)]^{1/2} = \Delta\left[\frac{\lambda u_0''}{2D}\right]^{1/2}. \tag{15}$$

The optimal section size Δ is found by taking the derivative of $(p_1 + p_2)$ with respect to Δ and setting the result to zero to yield

$$\Delta_{\text{opt}} = \lambda^{1/4} D^{3/4} (\tfrac{1}{2}u_0'')^{-1/4}. \tag{16}$$

Finally, the SBP capabilities are found by combining the results of approximations (14) and (15) with Eq. (16) to yield

$$N \approx D/(p_1 + p_2) \approx \lambda^{-3/4} D^{3/4} (\tfrac{1}{2}u_0'')^{-1/4}$$

$$= F^{3/4} (\tfrac{1}{2}u_0'')^{-1/4} \tag{17}$$

Approximation (17) implies that, up to a constant, the SBP capabilities of the proposed two-stage optical implementation of Fig. 3 have a power dependence of 3/4 in F, instead of a power dependence of only 1/2 for a general space-variant operation. Moreover the SBP capabilities are inversely proportional to the second derivative of the (normalized) CT function u_0''. This indicates that smoothness is indeed the symmetry that is exploited here, and CT's that are almost linear with low second derivatives should have higher SBP capabilities then those with high second derivatives. Of course the SBP capabilities cannot exceed F, so approximation (17) is valid only as long as the second derivative of the CT is not smaller than $2/F$.

VI. Concluding Remarks

The SBP capabilities of free-space optical interconnects were analyzed by applying Gabor's theory of information. It was shown that it is possible to exploit symmetry properties in order to increase the SBP capabilities. Two examples of obvious symmetries, locality and separability, were presented along with experimental results. Another less obvious symmetry, that of smoothness, was also described. We believe that the concept of the different types of operations could be further extended to include more hidden symmetries of the interconnect schemes and more sophisticated optical operations. This should lead to more efficient optical interconnect architectures that would be more suitable for optical implementation.

References

1. R. Barakat and J. Reif, "Lower bounds on the computational efficiency of optical computing systems," Appl. Opt. **26,** 1015–1018 (1987).
2. M. R. Feldman and C. G. Guest, "Interconnect density capabilities of computer generated holograms for optical interconnection of very large scale integrated circuits," Appl. Opt. **28,** 3134–3137 (1989).
3. M. R. Feldman, C. G. Guest, T. J. Drabik, and S. C. Esener, "Comparison between electrical and free space optical interconnects for fine grain processor arrays based on interconnect density capabilities," Appl. Opt. **28,** 3820–3829 (1989).
4. B. K. Jenkins, P. Chavel, R. Forchheimer, A. A. Sawchuck, and T. C. Strand, "Architectural implications of a digital optical processor," Appl. Opt. **23,** 3465–3474 (1984).
5. J. W. Goodman, "Linear space-variant optical data processing," in *Optical Information Processing,* S. H. Lee, ed. (Springer-Verlag, Berlin, Heidelberg, New York, 1981), p. 248.
6. D. Gabor, "Light and information," in *Progress in Optics,* E. Wolf, ed. (North-Holland, Amsterdam, 1961), Vol. 1, pp. 109–153.
7. O. Bryngdahl, "Geometrical transformation in optics," J. Opt. Soc. Am. **64,** 1092–1099 (1974).
8. G. Toraldo di Francia, "Super-gain antennas and optical resolving power," Nuovo Cimento Suppl. **9,** 426–435 (1952).
9. A. Harootunian, E. Betzig, A. Muray, A. Lewis, and M. Isaacson, "Near-field investigation of submicrometer apertures at optical wavelengths," J. Opt. Soc. Am. A **1,** 1293–1293 (1984).
10. K. W. Urquhart, P. Marchand, Y. Fainman, and S. H. Lee, "Design of free-space optical interconnection systems utilizing diffractive optics," in *Annual Meeting 1991,* Vol. 17 of OSA Technical Digest Series (Optical Society of America, Washington, D.C., 1991), p. 70.
11. S. Wolfram, *Theory and Applications of Cellular Automata,* (World Scientific, Singapore, 1986).
12. A. W. Lohmann, W. Stork, and G. Stucke, "Optical perfect shuffle," Appl. Opt. **25,** 1530–1531 (1986).
13. N. Davidson, A. A. Friesem, and E. Hasman, "Realization of perfect shuffle and inverse perfect shuffle transforms with holographic elements," Appl. Opt. (to be published).
14. J. Schwider, W. Stork, N. Streibl, and R. Volkel, "Possibilities and limitations of space-variant holographic optical elements for switching networks and general interconnects," in *Optics in Complex Systems,* F. Lanzl, H. Preuss, and G. Weigelt, eds., Proc. Soc. Photo-Opt. Instrum. Eng. **1319,** 130–131 (1990).
15. N. Davidson, A. A. Friesem and E. Hasman, "Optical coordinate transformations," Appl. Opt. **31,** 1067–1073 (1992).
16. G. E. Lohman and A. W. Lohmann, "Optical interconnection networks utilizing diffraction gratings," Opt. Eng. **27,** 893–900 (1988).
17. W. H. Lee, "Binary synthetic holograms," Appl. Opt. **13,** 1677–1682 (1974).